eLIFE
elifesciences.org

Figures and figure supplements

Sodium taurocholate cotransporting polypeptide is a functional receptor for human hepatitis B and D virus

Huan Yan, et al.

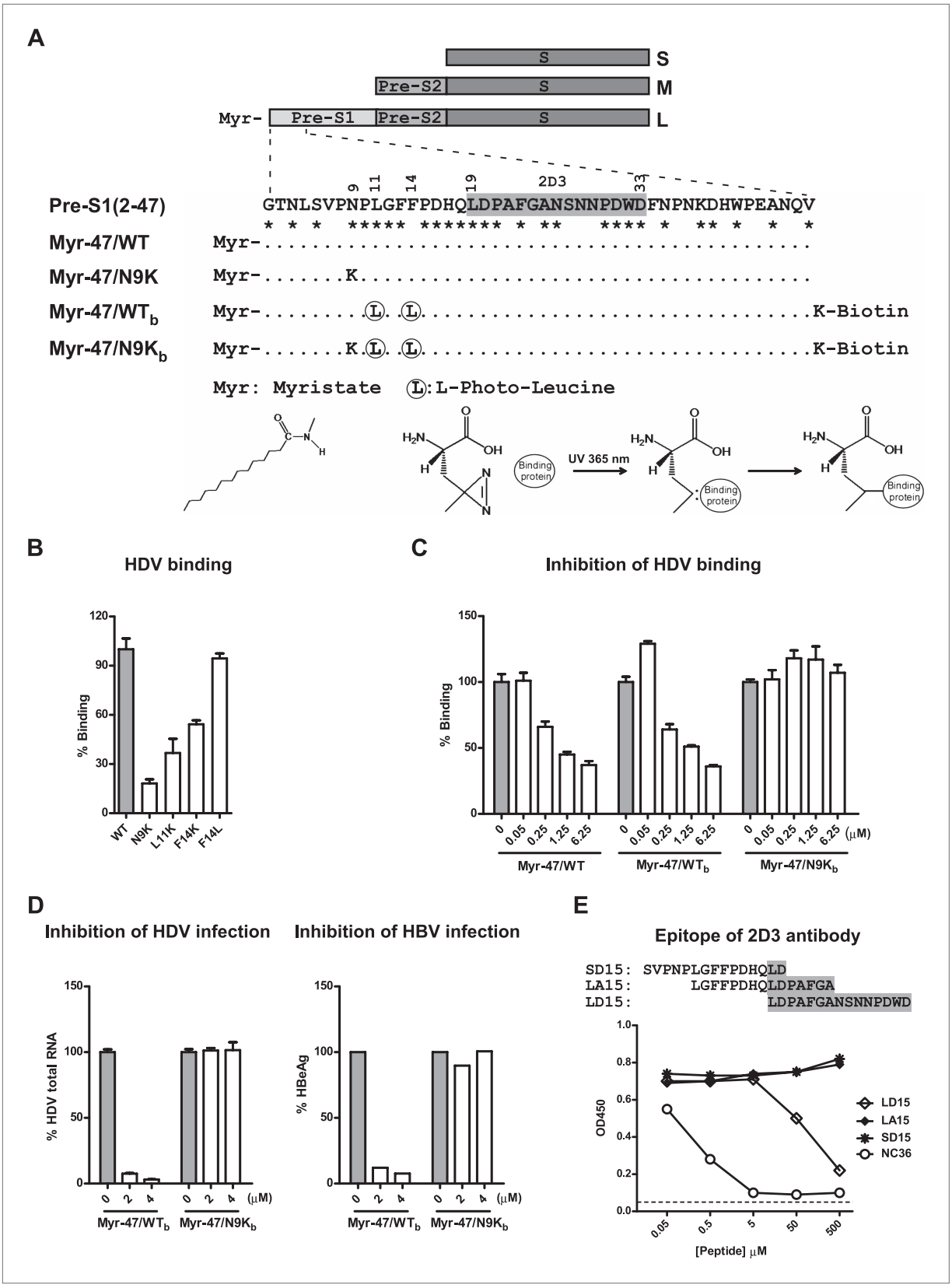

Figure 1. Developing photoreactive peptide ligands and an antibody for identifying pre-S1 binding partner(s) by zero distance cross-linking. (**A**) Schematic diagram of HBV envelope proteins and N-terminal peptides of pre-S1 domain. Pre-S1 (2-47): 2-47th residues of the pre-S1 domain of the L

Figure 1. Continued on next page

Figure 1. Continued

protein of HBV (S472 strain, genotype C). Residue numbering is based on genotype D. Asterisk indicates highly conserved residues among genotypes. Epitope of mAb 2D3 was shaded in gray. (**B**) Effect of alterations of the critical N-terminal residues within pre-S1 region of L protein on HDV binding to PTHs. Both wild-type (WT) and mutant HDV virions carry HBV envelope proteins. Mutant HDV carries point mutation as indicated in the pre-S1 region of L protein. PTHs were incubated with HDV at 16°C for 4 hr and followed by extensive wash; bound virions were quantified by qRT-PCR for virus genome RNA copy, and the data are presented as percentage of virus binding, the binding of WT virus was set as 100%. (**C**) Myr-47/WT_b bait peptide dose-dependently inhibited HDV virion binding. The binding assay was performed similarly as panel B except that PTHs were pre-incubated with indicated peptides. (**D**) Inhibition of viral infection by the photoreactive peptides. Left: PTHs were pre-incubated with peptides at indicated concentrations at 37°C for 1 hr and then inoculated with HDV virus. Viral infection was examined by measuring viral RNA in infected cells with qRT-PCR 6 days post-infection (dpi). Data are presented as percentage HDV infection. Right: peptides at indicated concentrations were added to PTHs before HBV inoculation. The cell culture medium was replenished every 2 days. Secreted viral antigen HBeAg was measured by ELISA on 6 dpi, and the data are presented as percentage of that in the absence of peptides. (**E**) Antibody 2D3 recognizes residues 19–33 of pre-S1. Peptide NC36 (aa 4–36 of pre-S1, NLSVPNPLGFFPDHQLDPAFGANSNNPDWDFNP) conjugated with keyhole limpet hemocyanin (KLH) was the immunogen peptide for generating mouse mAb 2D3. Binding activity of 2D3 with full-length pre-S1 protein was measured by ELISA in the presence of competition peptides at indicated concentrations. LD15 peptide compassing residues 19–33 of pre-S1 inhibited 2D3 binding in a dose-dependent manner, indicating that 2D3 recognizes an epitope within this region. HBV: hepatitis B virus; mAb: monoclonal antibody; HDV: hepatitis D virus; PTH: primary *Tupaia* hepatocytes; HBeAg: HBV e antigen.

DOI: 10.7554/eLife.00049.003

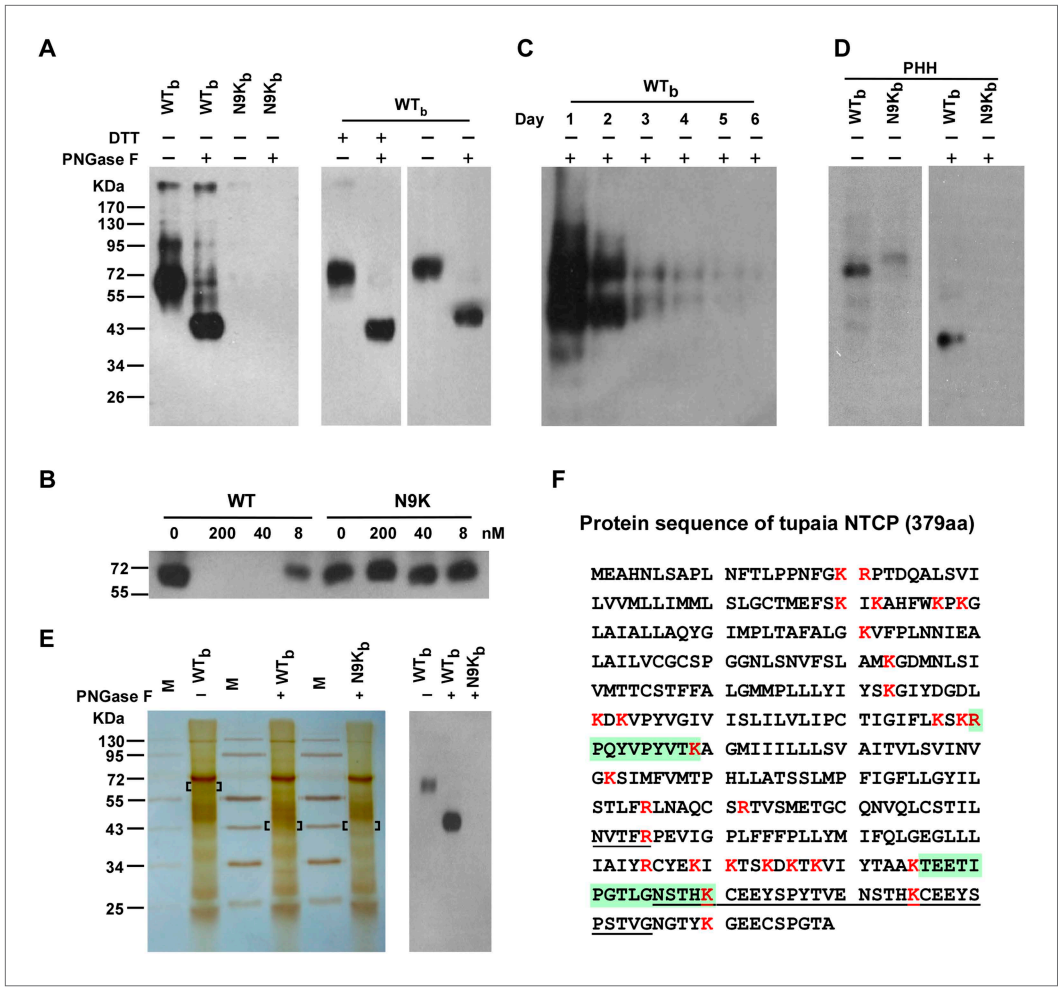

Figure 2. Identification of pre-S1 binding protein on primary hepatocytes with photoreactive peptide Myr-47/WT_b. (**A**) Left: Cultured PTHs at 24–48 hr after isolation and plating were photo-cross-linked with 200 nM Myr-47/WT_b (WT_b) or Myr-47/$N9K_b$ ($N9K_b$), followed by Streptavidin Dynal T1 beads precipitation and Western blot analysis using mAb 2D3. The protein cross-linked by WT_b is sensitive to PNGase F treatment and shifted from ~65 to ~43 kDa. Right: WT_b cross-linked samples were treated with 100 mM DTT and/or PNGase F as indicated and detected similarly as in the left panel. (**B**) Non-photoreactive Myr-47/WT peptide (WT) but not its N9K mutant competed with 200 nM of WT_b peptide for cross-linking with PTHs in a dose-dependent manner. (**C**) The abundance of the target protein(s) in PTH cells decreased over time. PTHs on different days of in vitro culturing were photo-cross-linked with 200 nM WT_b. The cross-linked samples were analyzed by Western blot. The two bands at ~65 and ~43 kDa were due to incomplete deglycosylation by PNGase F. (**D**) WT_b cross-linking with primary human hepatocytes (PHH). Frozen PHH cells were thawed and plated 1 day before cross-linking. With same procedure as in panel A, 200 nM WT_b but not $N9K_b$ cross-linked with a glycoprotein of molecular weight at ~60 kDa, which shifted to ~39 kDa upon PNGase F treatment. (**E**) Purification of target protein(s) for MS analysis. PTHs photo-cross-linked with 200 nM of WT_b or $N9K_b$ peptide were lysed, then the peptides and their cross-linked proteins were purified in tandem with Streptavidin Dynal T1 beads, mAb 2D3 conjugated beads, and Streptavidin Dynal T1 beads in 1× RIPA buffer. Extensive wash was applied for each purification step. The samples were treated with or without PNGase F as indicated prior to the last step of Streptavidin beads precipitation. The final purified samples were subjected to SDS-PAGE followed by silver staining (left). Bracketed areas indicate the bands cut for MS analysis. Western blot analysis (right) of the same cross-linked samples were performed similarly as in panel A. The top 10 nonredundant proteins identified in the 3 samples by MS analysis are listed in Figure 2—Source data 1. The common protein hit identified by MS analysis of the ~65- and ~43-kDa bands cut from the WT_b cross-linked sample was *Tupaia* NTCP (tsNTCP), and the representative MS/MS spectra and parameters of the peptide hits are shown in ***Figure 2—figure supplement 5***. The control band cut from $N9K_b$ cross-linked sample did not generate any hits on any of these peptides. (**F**) Predicted tsNTCP protein sequence. A 30-amino acid insertion unique to

Figure 2. Continued on next page

Figure 2. Continued

tsNTCP is underlined. Two peptides identified by LC-MS/MS were highlighted in green. All lysine and arginine are highlighted in red to indicate trypsin cleavage sites. Many of the potential tryptic peptides are not appropriate for LC-MS detection because of unfavorable size and/or hydrophobicity. PTH: primary *Tupaia* hepatocytes; MS: mass spectrometry.

DOI: 10.7554/eLife.00049.004

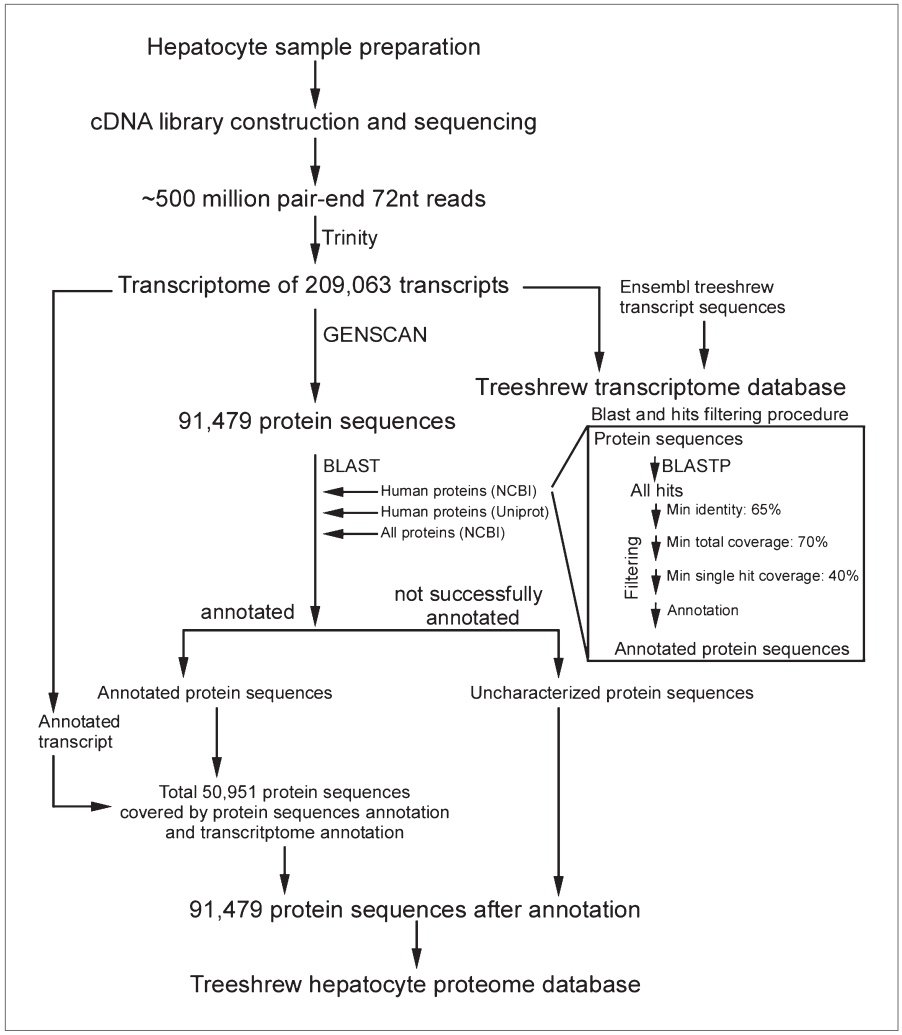

Figure 2—figure supplement 1. Generation of *Tupaia* hepatocytes proteome database from Illumina deep sequencing-determined transcriptome of PTHs. Workflow chart of bioinformatics analysis of Illumina deep sequencing-determined transcriptome of *Tupaia* hepatocytes and generation of protein sequence database of PTH.

DOI: 10.7554/eLife.00049.006

Tupaia hepatocyte transcriptome and proteome assembly		
RNA-seq statistics (72nt pair-end sequencing)		
Sequencing reads	Library 1	75,283,002
	Library 2	57,658,056
	Library 3	84,228,832
	Library 4	83,296,198
	Library 5	84,192,426
	Library 6	78,866,948
	Library 7	76,454,126
Transcriptome and proteome assembly		
Total reads number		539,979,588
Total base number (Gbase)		38.9
Transcripts number		209,063
Transcripts average length (nt)		1,421
Transcripts N50 length (nt)*		3,674
Transcripts maximum length (nt)		21,043
Transcripts with full length cDNA#		15,545
Predicted protein number		91,479
Annotated protein number		50,951

Figure 2—figure supplement 2. Generation of *Tupaia* hepatocytes proteome database from Illumina deep sequencing-determined transcriptome of PTHs. Statistics of outputs in generation of *Tupaia* hepatocytes proteome database.

DOI: 10.7554/eLife.00049.007

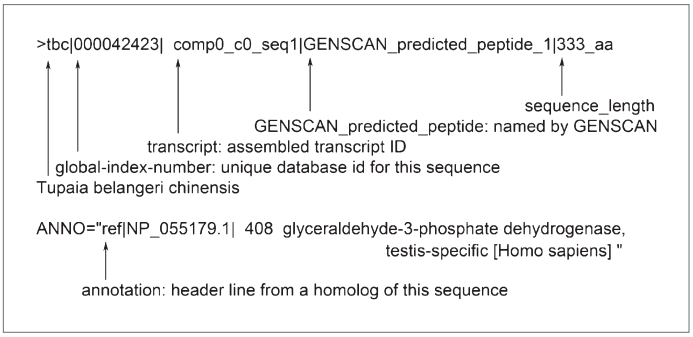

Figure 2—figure supplement 3. Generation of *Tupaia* hepatocytes proteome database from Illumina deep sequencing-determined transcriptome of PTHs. Format of *Tupaia* hepatocyte proteome database. Head of *Tupaia* protein sequence for glyceraldehyde-3-phosphate dehydrogenase (GAPDH) in FASTA file was shown as an example. The *Tupaia* hepatocyte proteome database with 91,479 sequences was stored in FASTA file in a supplementary database. The FASTA sequence header lines show information about the generation procedures of these sequences and the functional annotations of their homolog(s).

DOI: 10.7554/eLife.00049.008

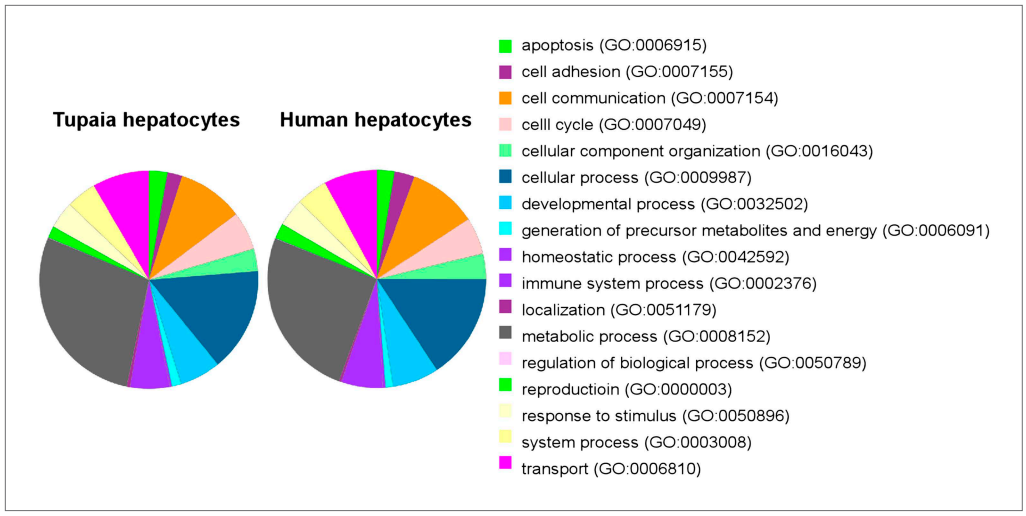

Figure 2—figure supplement 4. Generation of *Tupaia* hepatocytes proteome database from Illumina deep sequencing-determined transcriptome of PTHs. Pie charts of genes expressed in primary hepatocytes of *Tupaia* and human. PANTHER database (***Mi et al., 2005***) was used to determine the Gene Ontology (GO) biological process distribution of annotated transcripts and protein sequences of primary *Tupaia* hepatocytes and that of primary human hepatocytes reported by ***Hart et al. (2010)***. Major human hepatocyte protein classes are represented in the *Tupaia* hepatocytes proteome database generated in this study.

DOI: 10.7554/eLife.00049.009

A

65 kDa - WT_b/PNGaseF (-)

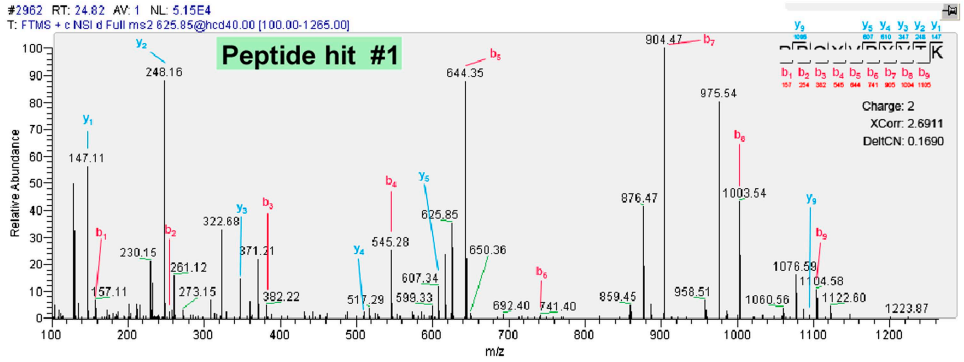

Sample	WT_b/ PNGaseF(-)
Charge	+2
X corr	2.6911
Delt CN	0.169
Obs M^+H^+	1250.6882
Calc M^+H^+	1250.6892
PPM	-0.8

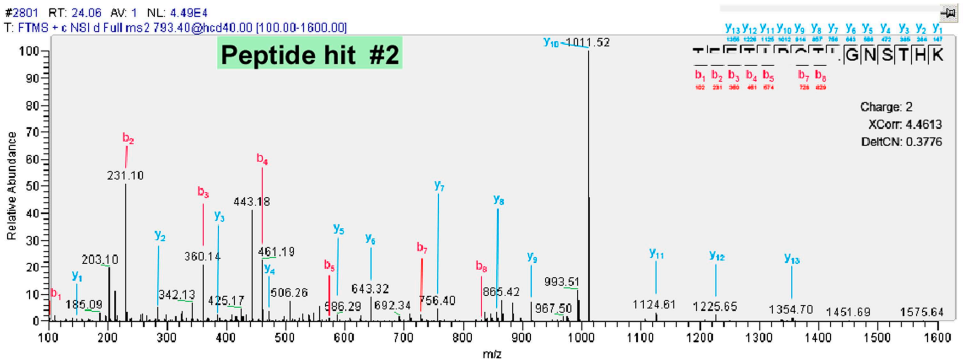

Sample	WT_b/ PNGaseF(-)
Charge	+2
X corr	4.4613
Delt CN	0.3776
Obs M^+H^+	1585.7885
Calc M^+H^+	1584.7864
PPM	-0.8

B

43 kDa - WT_b/PNGaseF (+)

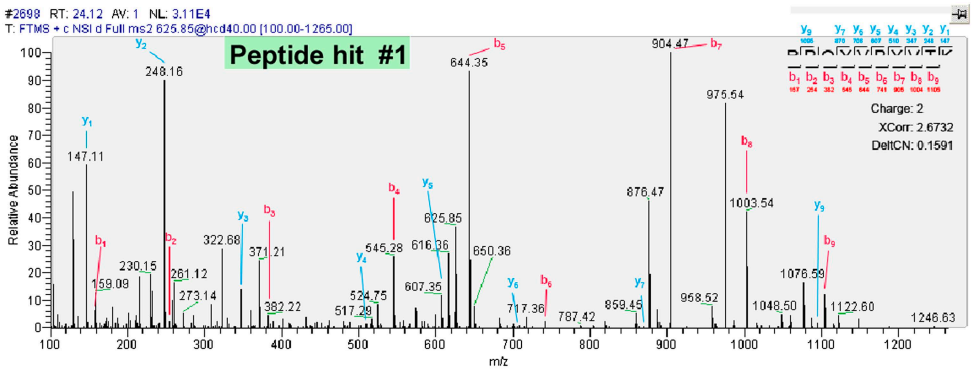

Sample	WT_b/ PNGaseF(+)
Charge	+2
X corr	2.6732
Delt CN	0.1591
Obs M^+H^+	1250.6876
Calc M^+H^+	1250.6892
PPM	-1.3

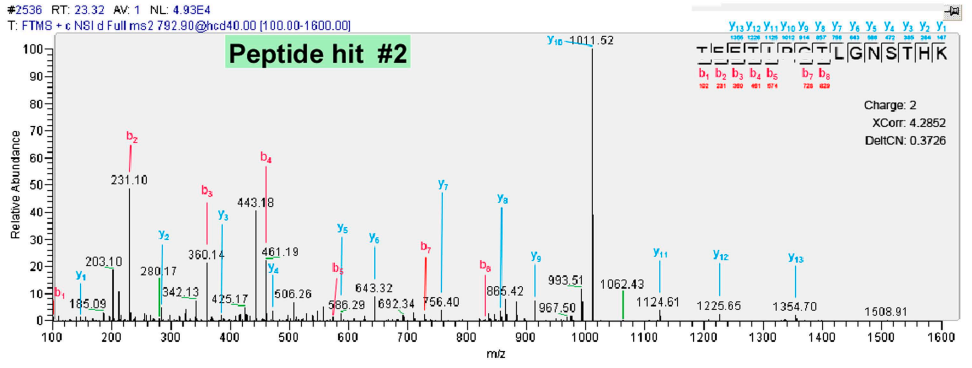

	WT_b/ PNGaseF(+)
Charge	+2
X corr	4.2852
Delt CN	0.3726
Obs M^+H^+	1584.7859
Calc M^+H^+	1584.7864
PPM	-0.3

Figure 2—figure supplement 5. Representative MS/MS spectra and parameters of the identified peptide hits. The (**A**) ~65- and (**B**) ~43-kDa bands cut from the WTb cross-linked sample (***Figure 2E***, left) were analyzed by mass spectrometry. The MS/MS spectra and parameters of the NTCP peptide hits are shown.

DOI: 10.7554/eLife.00049.010

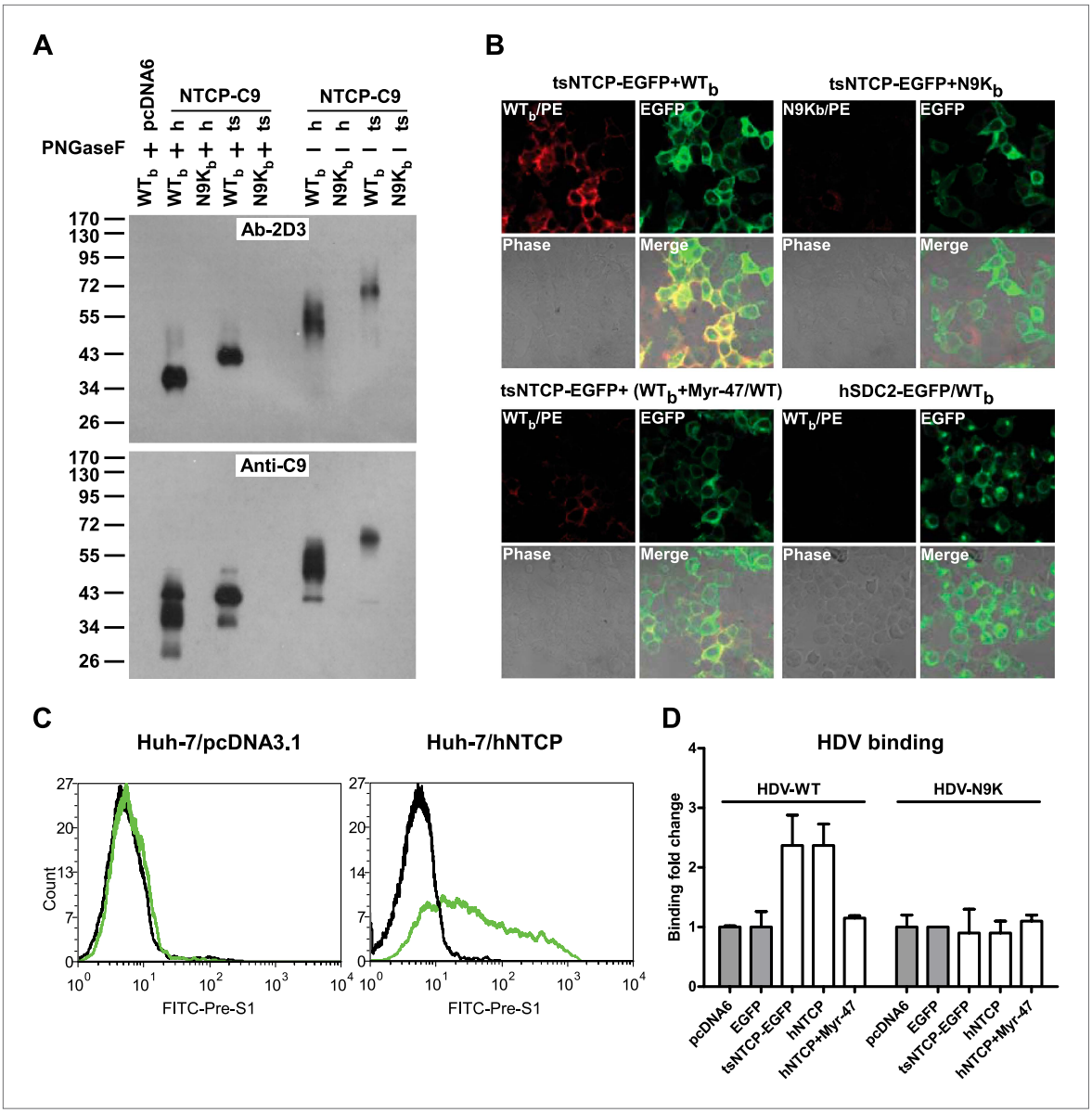

Figure 3. Binding of NTCP with N-terminal peptide of pre-S1 and HDV virions. (**A**) 293T cells transfected with an expression vector or plasmid containing cDNA of h*NTCP* or ts*NTCP* fused with a C9 tag at its C-terminus were cross-linked with 200 nM Myr-47/WT_b or Myr-$N9K_b$ similarly as in ***Figure 2A*** at 24 hr post-transfection. Cross-linked protein samples were precipitated by Streptavidin Dynal beads followed by treatment with PNGase F as indicated, and then analyzed by Western blotting using mAb 2D3 or anti-C9 tag antibody. (**B**) 293T cells transfected with tsNTCP-EGFP or a control hSDC2-EGFP (encoding human heparan sulfate proteoglycan core protein fused with EGFP at C-terminus) expression plasmid were incubated with WT_b or $N9K_b$ in the presence or absence of 200 nM non-photoreactive Myr-47/WT as indicated. Bound peptides were probed with PE-streptavidin and the colocalization of peptide and NTCP on cell surface was shown in the merged images. (**C**) FACS analysis of pre-S1 peptide binding with hNTCP transiently transfected Huh-7 cells. 24 hr post-transfection with hNTCP or a control plasmid, the cells were stained with 200 nM FITC-pre-S1 (FITC-labeled lipopeptide corresponding to the N-terminal 59-amino acid of pre-S1). The binding was analyzed by flow cytometry. (**D**) Huh-7 cells, after 24 hr of transfection of indicated plasmids, were incubated with wild-type HDV or HDV with a N9K mutation on its L protein. Bound virions were quantified by qRT-PCR. The result is presented as fold changes of binding over the background virus binding to pcDNA6-transfected cells. mAb: monoclonal antibody; tsNTCP: *Tupaia* NTCP; NTCP: sodium taurocholate cotransporting polypeptide.

DOI: 10.7554/eLife.00049.011

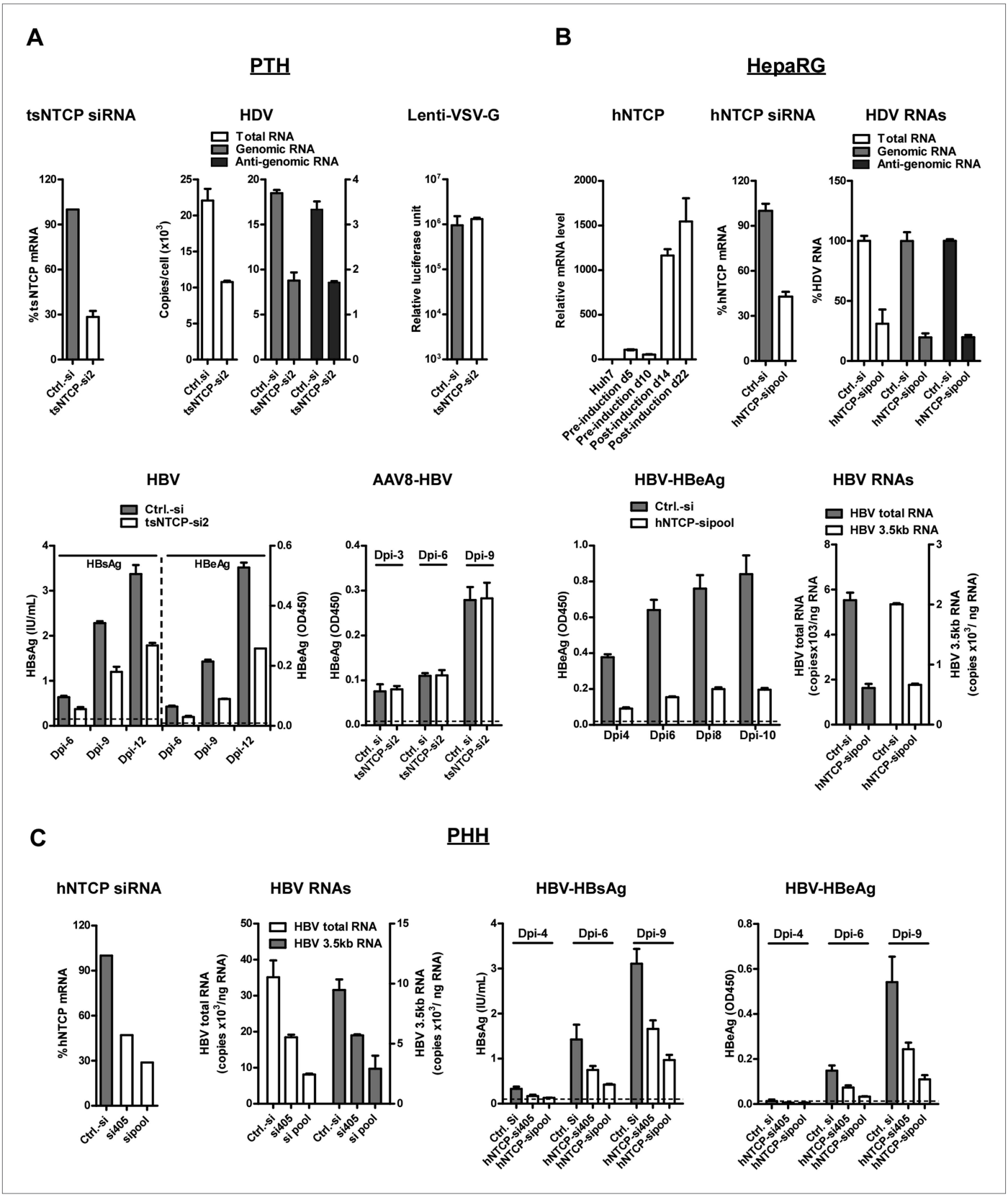

Figure 4. HDV and HBV infections of hepatocytes require NTCP. (**A**) Infections of HDV and HBV in PTHs were inhibited by tsNTCP knockdown. Freshly isolated PTHs were transfected with siRNAs against tsNTCP or a control siRNA. 3 days later, 1 × 10^5 PTHs were inoculated with HDV, HBV, or control

Figure 4. Continued on next page

Figure 4. Continued

viruses AAV8-HBV and Lenti-VSV-G. For HDV and HBV, PTHs were infected at 500 and 100 genome equivalent copies per cell, respectively. The level of HDV viral RNAs in infected cells was quantified by qRT-PCR on 6 dpi. Strand-specific primers were used to differentiate the HDV genomic and antigenomic RNAs (see 'Materials and methods'). For VSV-G control virus infection, recombinant lentivirus pseudotyped by VSV-G carrying a luciferase reporter was inoculated to PTHs 3 days after siRNA transfection. The luciferase activity was assessed on 6 dpi. For HBV infection, the kinetics of secreted viral antigens HBsAg and HBeAg were measured by ELISA. The medium was changed every 3 days. For AAV8-HBV infection, PTHs were infected with a recombinant AAV8 carrying 1.05× overlength HBV genome. Secreted HBeAg was assessed on indicated days post-infection. The effect of tsNTCP silencing in all viral infections was independently evaluated with a total of four siRNAs against tsNTCP (see 'Materials and methods'). The data shown are the result of a representative siRNA out of the four tested. (**B**) Differentiated HepaRG cells express high level of NTCP mRNA and knockdown NTCP in these cells inhibited HDV and HBV infections. HDV and HBV infection of siRNA-transfected HepaRG cells was conducted similarly as in panel A. HDV RNA levels in the infected cells were measured on 9 dpi. For HBV infection, secreted HBeAg was collected every 2 days as indicated and analyzed by ELISA. The copy numbers of HBV total RNA and 3.5 kb RNA in the infected cells were measured at the end of the experiment, 10 dpi. (**C**) Knockdown hNTCP in PHHs hampered HBV infection. Frozen PHHs were thawed and plated 1 day before transfecting with siRNAs against hNTCP or a control siRNA. Similar to panels A and B, 3 days after transfection, PHHs were inoculated with 100 genome equivalent copies of HBV per cell, and the levels of secreted HBeAg were determined at indicated dpi. HBV RNAs were quantified at the end of the experiment, 9 dpi. The knockdown efficiency of siRNA targeting tsNTCP or hNTCP shown in panels A–C was determined by real time RT-PCR on day 4 after transfection. NTCP: sodium taurocholate cotransporting polypeptide; HBV: hepatitis B virus; HDV: hepatitis D virus; PTH: primary *Tupaia* hepatocytes; tsNTCP: *Tupaia* NTCP; siRNA: small interfering RNA; dpi: days post-infection; hNTCP: human NTCP.

DOI: 10.7554/eLife.00049.012

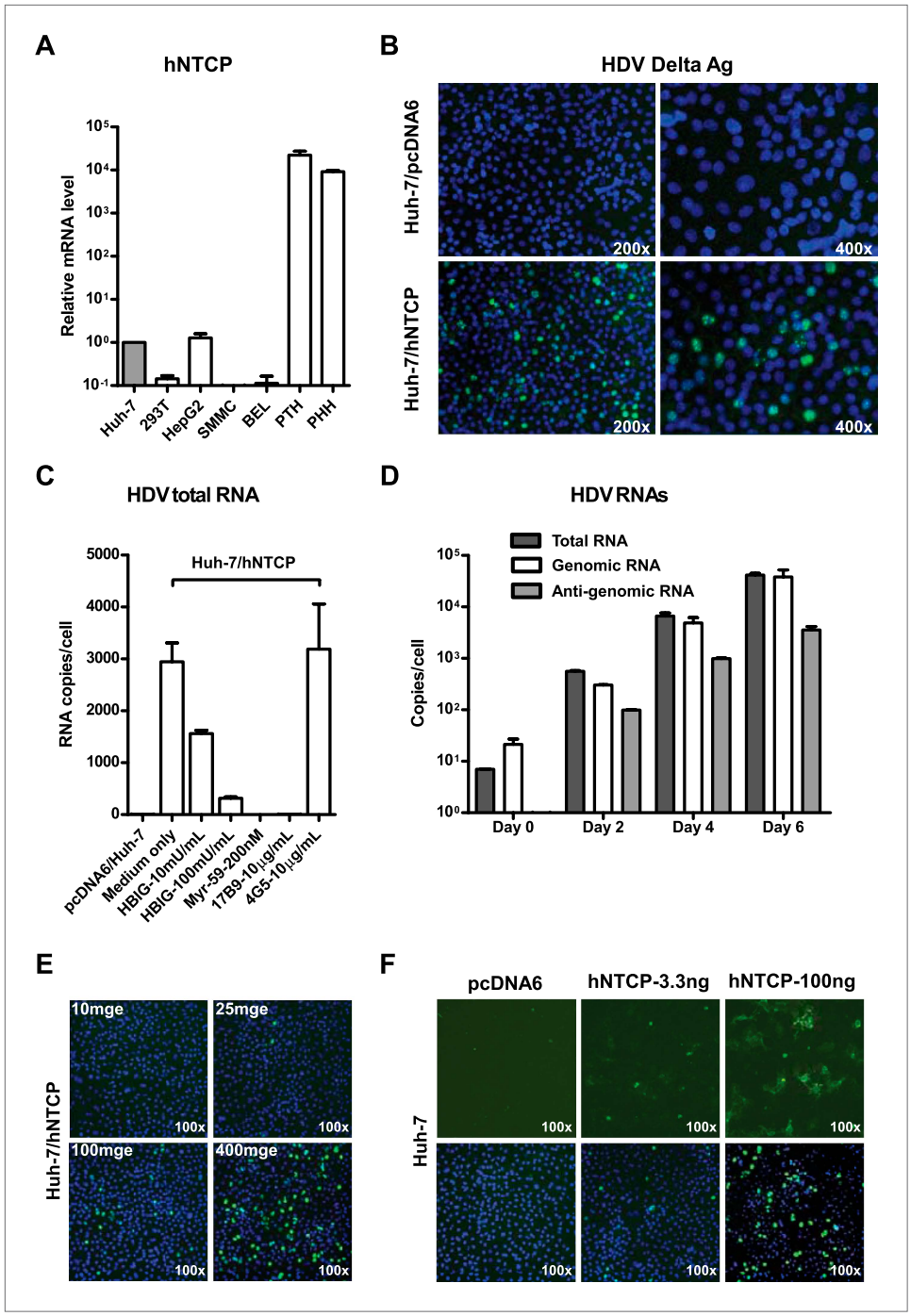

Figure 5. NTCP expression confers Huh-7 susceptibility to HDV infection. (**A**) NTCP mRNA expression level in the indicated cell lines and primary hepatocytes. The Huh-7 was used to normalize the relative expression levels in other cells. (**B**) 1 × 10^5 Huh-7 cells were transfected with 100 ng hNTCP/pcDNA6 or a vector control in 24-well plate and maintained in PMM, 24 hr after transfection, transfected cells were infected with HDV at 500 genome equivalent copies per cell. On 8 dpi, HDV delta antigen, which typically locates in nuclei, was stained with 4G5 antibody in green, nuclei were stained with DAPI in blue. (**C**) Huh-7 cells transfected with hNTCP were infected with HDV similarly as in panel B in the presence or absence of HBV entry inhibitors: HBIG (hepatitis B immune globulin), Myr-59, and anti-HBsAg mAb, 17B9. 4G5 was used as an antibody control. HDV RNA copies of infected cells were quantified by real-time RT-PCR on 6 dpi. (**D**) Huh-7 cells transfected with hNTCP were infected with HDV similarly as in panel B. The HDV viral RNAs in infected cells at indicated time points were quantified by real-time RT-PCR. (**E**) HDV infection with increasing multiplicities of genome equivalents (mge). With 100 ng hNTCP/pcDNA6, 1 × 10^5

Figure 5. Continued on next page

Figure 5. Continued

Huh-7 cells were transfected, as in panel B. Transfected cells were infected with increasing mge of HDV as indicated. HDV delta antigen was detected as in panel B on 8 dpi. (**F**) HDV infection of cells with increasing levels of hNTCP. About 1 × 10^5 Huh-7 cells were transfected with a vector pcDNA6 or hNTCP/pcDNA6 at indicated amounts and cells were inoculated with 500 mge of HDV. HDV delta antigen was detected on 8 dpi as in panel B. NTCP: sodium taurocholate cotransporting polypeptide; PMM: primary hepatocytes maintenance medium; HBV: hepatitis B virus; HDV: hepatitis D virus; mAb: monoclonal antibody; HBsAg: HBV S antigen.

DOI: 10.7554/eLife.00049.013

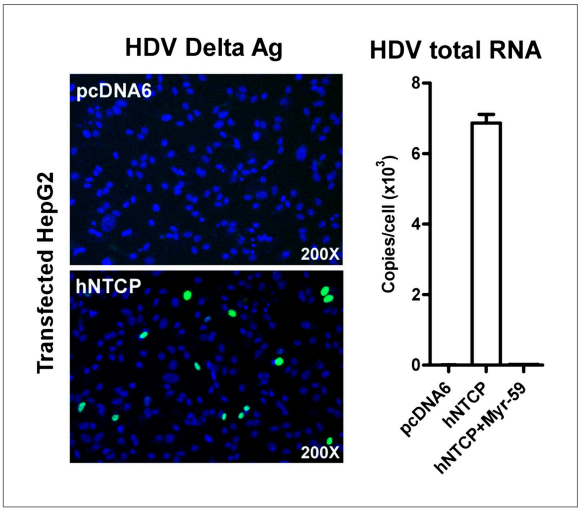

Figure 5—figure supplement 1. Infection of HDV on HepG2 cells expressing hNTCP. About 2 × 105 HepG2 cells were transiently transfected with 0.3 μg hNTCP/pcDNA6 or a vector control and maintained in PMM. Cells were infected at 500 mge with HDV 24 hr after transfection. On 8 dpi, HDV delta antigen in infected cells was stained with mAb 4G5 (left) and the HDV viral RNAs were determined by real time RT-PCR. The competing Myr-59 peptide was tested at 200 nM (right).

DOI: 10.7554/eLife.00049.014

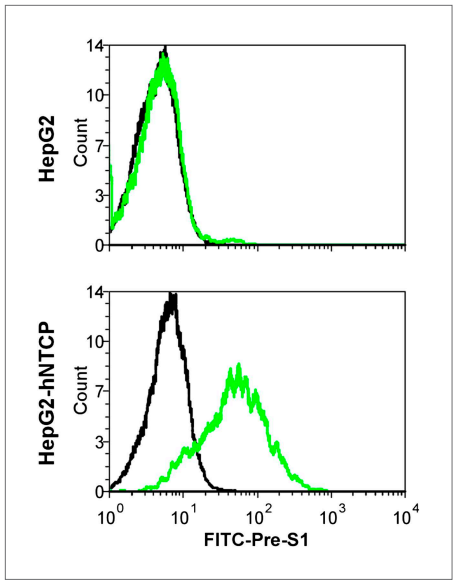

Figure 5—figure supplement 2. Infection of HDV on HepG2 cells expressing hNTCP. HepG2 stable cell line stably expressing hNTCP (HepG2-hNTCP) was established by G418 selection after transient transfection. The expression of hNTCP was confirmed by staining with FITC-pre-S1 peptide.

DOI: 10.7554/eLife.00049.015

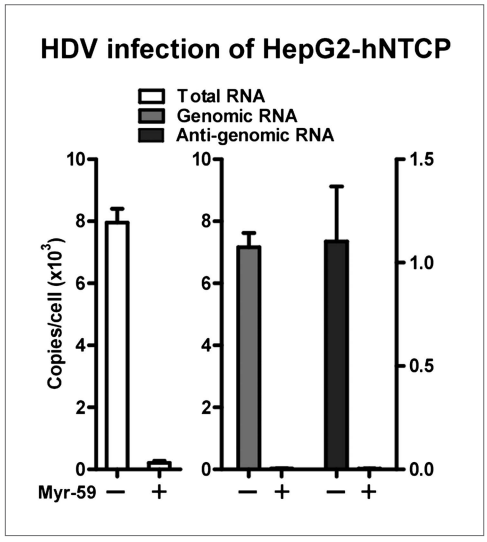

Figure 5—figure supplement 3. Infection of HDV on HepG2 cells expressing hNTCP. Infection of HDV on HepG2-hNTCP stable cells was conducted in the presence or absence of entry inhibitor 200 nM Myr-59. HDV total RNA, HDV genomic RNA, and antigenomic RNA were assayed with real time qPCR on 8 dpi.

DOI: 10.7554/eLife.00049.016

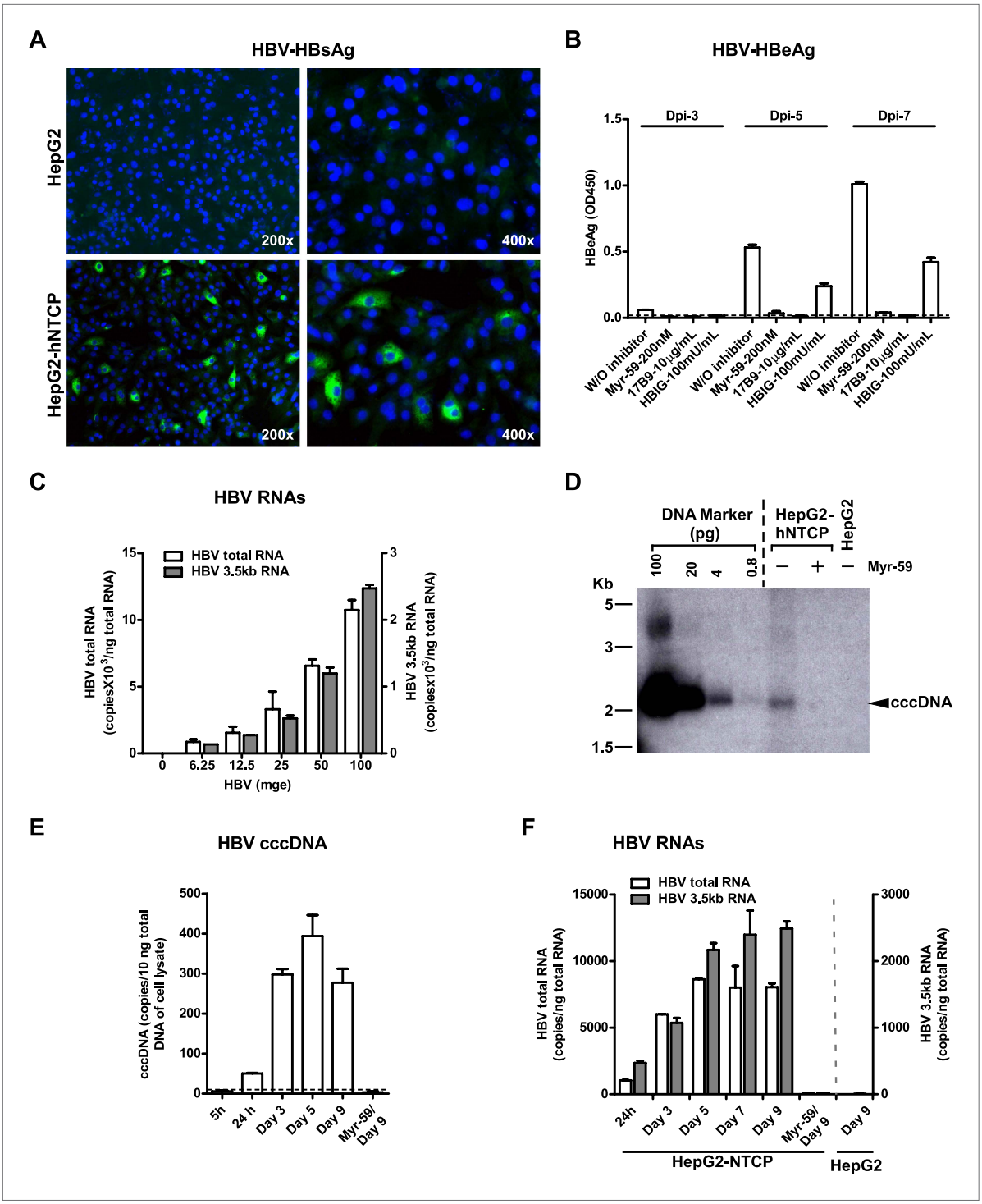

Figure 6. NTCP expression confers susceptibility to HBV infection. (**A**) Intracellular HBsAg expression in HBV-infected cells. HepG2-hNTCP stable cells or parental HepG2 cells were inoculated with HBV at 100 mge. On 9 dpi, intracellular HBsAg of infected cells on coverslips was stained with antibody 17B9 in green, and nuclei were stained with DAPI in blue. (**B**) Secreted HBeAg levels in the supernatants of HBV-infected cells. The cells were infected with HBV at 100 mge in the presence or absence of entry inhibitors as indicated. The medium was changed every 2 days. Secreted HBeAg was measured at 3, 5, 7 dpi; each time point represents the level of newly synthesized HBeAg within every 2 days. (**C**) HBV infection efficiency is correlated with the viral inoculum dose. With increasing dose of HBV, 2×10^5 HepG2-hNTCP cells were infected as indicated. HBV RNAs in infected cells was examined on 10 dpi with real-time RT-PCR for the total HBV RNAs and the 3.5 kb transcripts. (**D**) Southern blot analysis of cccDNA. HepaG2-hNTCP cells or HepG2 parental cells were infected with 100 mge of HBV in the presence or absence of Myr-59. HBV cccDNA was extracted from ~ 2–3 × 10^6 infected cells on 7

Figure 6. Continued on next page

Figure 6. Continued

dpi. Half of the extracted DNA of each sample was subjected to a 1.3% agarose gel and analyzed by Southern blotting. A plasmid DNA marker for cccDNA (see 'Materials and methods') at different concentrations from 0.8 to 100 pg was included in the same gel. (**E**)–(**F**) Kinetic analysis of HBV cccDNA and RNAs in HBV-infected HepG2-hNTCP cells. HBV cccDNA (in panel E) was quantified at indicated time points post infection (see 'Materials and methods'). A dotted line indicates the background amplification. HBV RNA copies (in panel F) in the infected cells were measured at indicated time points, data of similarly infected parental HepG2 cells on 9 dpi were also shown. NTCP: sodium taurocholate cotransporting polypeptide; HBV: hepatitis B virus; HBsAg: HBV S antigen; HBeAg: HBV e antigen; mge: multiplicities of genome equivalents; dpi: days post-infection; cccDNA: covalently closed circular DNA; hNTCP: human NTCP.

DOI: 10.7554/eLife.00049.017

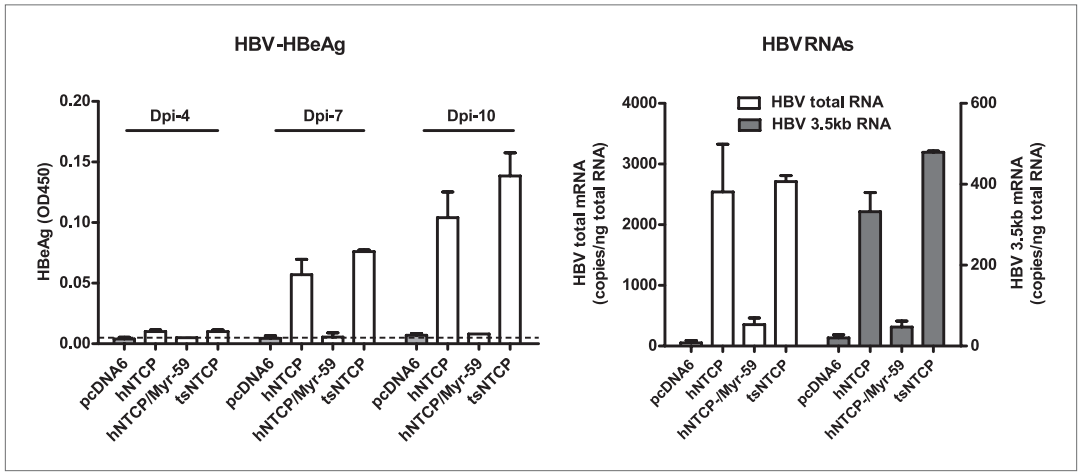

Figure 6—figure supplement 1. NTCP expression confers susceptibility to HBV infection. With 0.3 μg human or *Tupaia* NTCP/pcDNA6, or a vector control, 2×10^5 HepG2 cells were transiently transfected. The transfected cells were maintained in PMM. 24 hr after transfection, the cells were infected with HBV in the presence or absence of Myr-59 peptide (200 nM) as indicated at mge 100. Secreted viral HBeAg was examined with ELISA on days 4, 7, and 10 post-infection. HBV RNAs in infected cells was examined on 10 dpi for the total HBV RNAs or the 3.5 kb transcripts by real-time RT-PCR.

DOI: 10.7554/eLife.00049.018

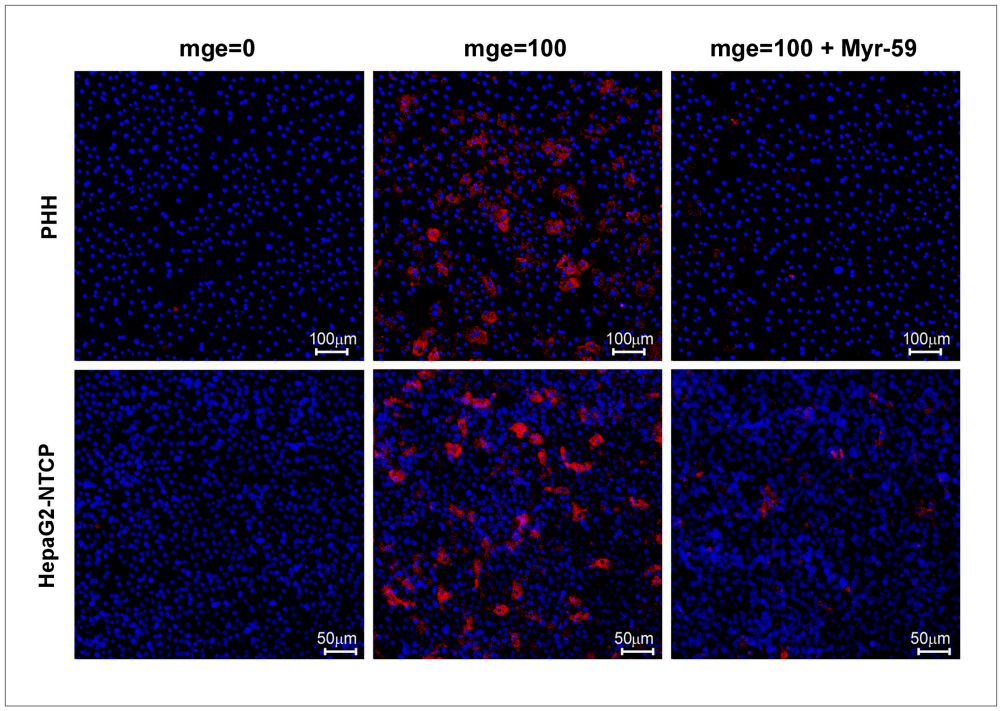

Figure 6—figure supplement 2. Comparative HBV infection of PHHs and HepG2-NTCP cells. PHHs from two donors (donor 1 and 2) or HepG2-NTCP cells in 48-well plate were infected with 100 HBV mge for 16 hr in the presence or absence of Myr-59 (200 nM). Same cells without viral inoculation were included as controls. The culture media were replenished every 2–3 days. On 8 days post-infection, the cells were fixed with 4% PFA, then stained for intracellular HBcAg with 5 μg/mL of anti-HBcAg-specific mAb 1C10, followed by Qdot 655 VIVID donkey anti-mouse IgG. HBcAg (red); nuclei (blue). The HBcAg staining images of PHHs from donor 1 are shown, which had higher infection efficiency than donor 2.

DOI: 10.7554/eLife.00049.019

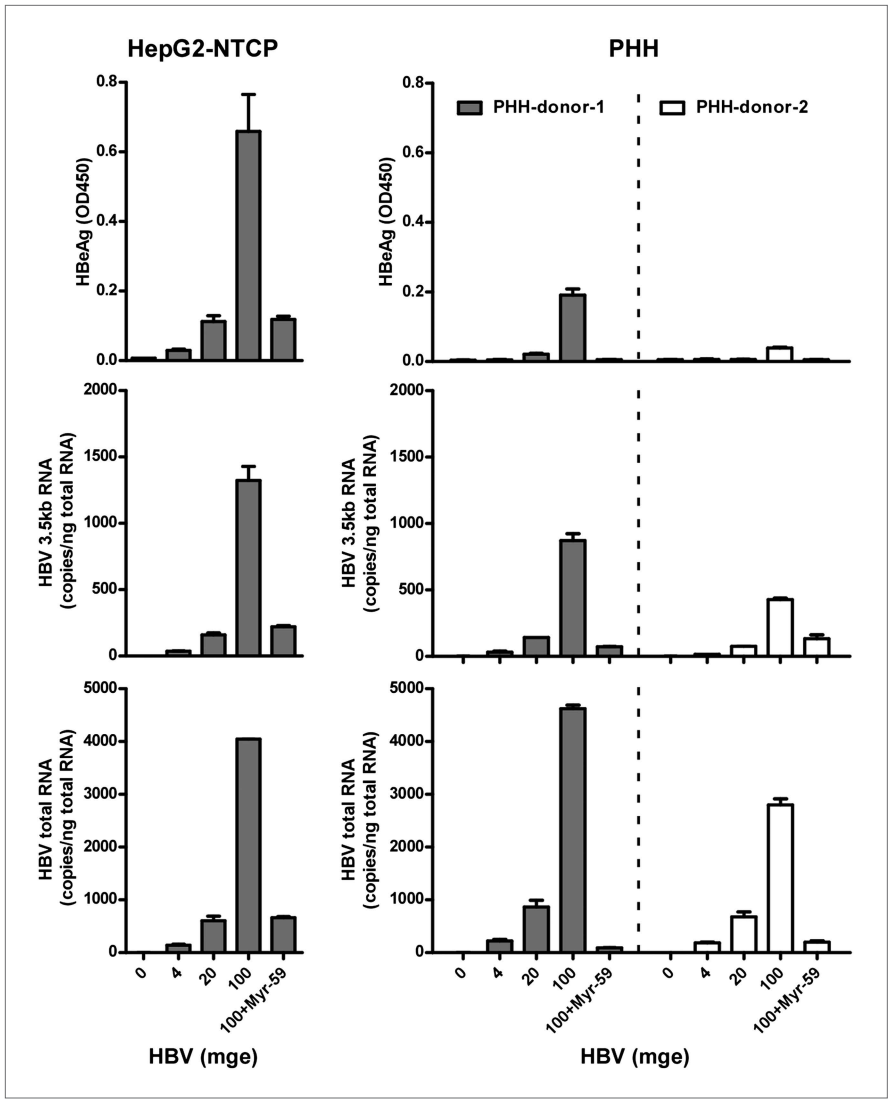

Figure 6—figure supplement 3. Comparative HBV infection of PHHs and HepG2-NTCP cells. HepG2-NTCP cells were infected as in ***Figure 6—figure supplement 2*** with 0, 4, 20, 100 mge of HBV for 16 hr. On 8 dpi, secreted HBeAg was examined by ELISA; intracellular HBV-specific RNAs were quantified with real-time RT-PCR. PHHs (donor 1 and 2) were infected and examined in parallel.

DOI: 10.7554/eLife.00049.020

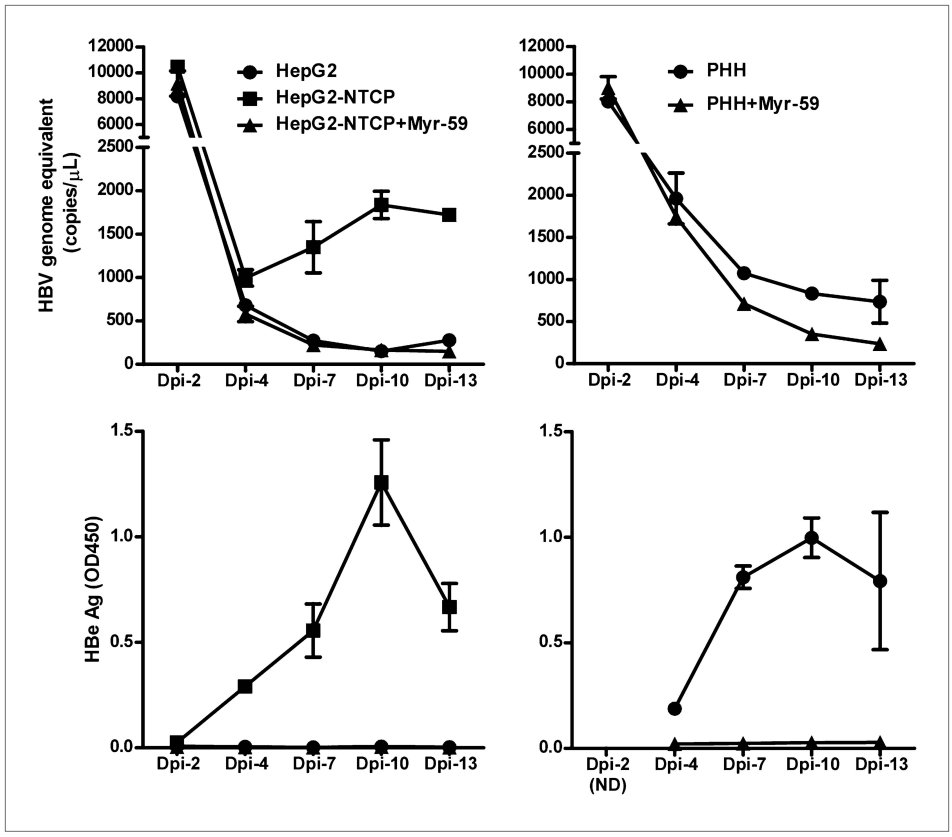

Figure 6—figure supplement 4. Kinetics of HBV viral DNA in the culture medium of primary infection and reinfection of the released viruses on PHHs. Kinetics of viral DNA in the culture medium of infected cells. Cells were plated in 48-well plate 1 day prior to infection, 1.5×10^5 HepG2 or HepG2-NTCP cells (left) and 7.5×10^4 attached PHHs (right) were infected in duplicate wells for 16 hr with 3.5×10^7 copies of HBV genome equivalent (genotype D) in a final volume of ~200 μl per well, respectively. The culture media were harvested and refreshed every 2–3 days for viral DNA and HBeAg measurement. Upper-left: the levels of HBV DNA in all three groups, HepG2, HepG2-NTCP, and HepG2-NTCP, in the presence of 200 nM Myr-59 peptide blocker, drastically declined on 4 dpi. For the control infection in HepG2 cells, the levels of viral DNA continuously declined throughout the remaining testing period to ~200 copies pe micorliter on 13 dpi. In contrast, viral DNA in the medium of infected HepG2-NTCP cells increased after the sharp decline on 4 dpi, reached to a maximum of 1.8×10^3 copies per microliter on 10 dpi, which was specifically inhibited by the entry inhibitor Myr-59 peptide. Upper-right: HBV DNA levels from infected PHH cultures in the presence or absence of Myr-59 peptide continuously decreased after a sharp drop on 4 dpi. However, in the absence of Myr-59, the viral DNA levels were two- to threefolds higher than that in the presence of Myr-59 from 7 to13 dpi. Bottom: significant HBeAg secretion was detected in HBV-infected HepG2-NTCP cells but not in the control HepG2 group and the group of HepG2-NTCP in the presence of Myr-59 (bottom-left). Efficient HBeAg secretion also was detected in PHH cultures in the absence of myr-59 peptide (lower-right).

DOI: 10.7554/eLife.00049.021

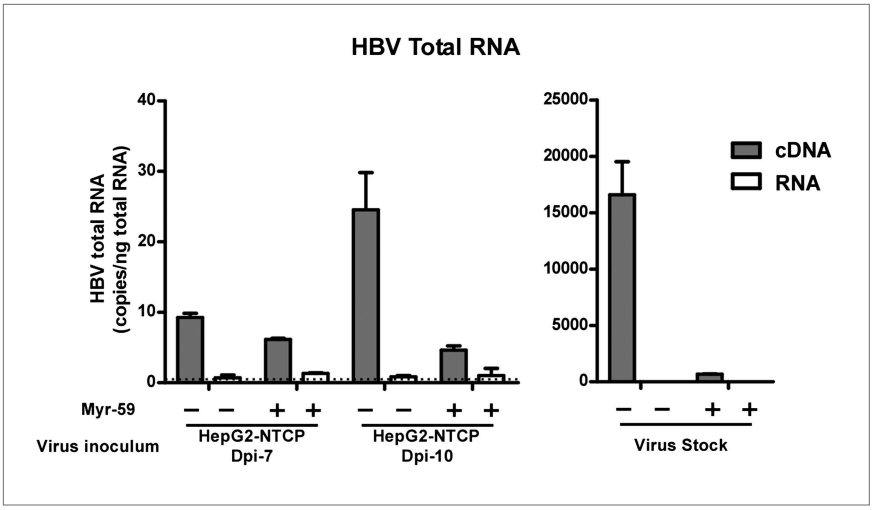

Figure 6—figure supplement 5. Kinetics of HBV viral DNA in the culture medium of primary infection and reinfection of the released viruses on PHHs. PHH infection assay of HBV progeny viral particles released from infected NTCP-expressing HepG2 cells. 200 μl of culture medium collected from HBV-infected HepG2-NTCP cells on 7 or 10 dpi were added to 7.5×10^4 PHH 1 day after cell plating, incubated at 37°C for 16 hr in the presence or absence of 200 nM Myr-59 peptide (left), followed by washing the cells and refreshing medium every 2–3 days. HBV RNAs were quantified with real-time RT-PCR on day 13 post-infection. The levels of HBV-specific 3.5 kb RNA was below detection limit (data not shown). Intracellular HBV total RNA was detected in PHHs inoculated with culture media that were collected from infected HepG2-NTCP cells on both 7 and 10 dpi, containing 2.7×10^5 and 3.6×10^5 copies genome equivalent viral DNA, respectively. As a control, same PHHs were infected with 500 mge HBV and the intracellular viral total RNA was determined on 13 dpi (right). cDNA: PCR amplification using cDNA templates that were reverse transcribed from cellular total RNA; RNA: PCR amplification with cellular total RNA without reverse transcription step, representing the background amplification of viral DNA contamination in the RNA preparation. Dotted line: detection limit of HBV total RNA per nanogram total RNA with real-time RT-PCR assay.

DOI: 10.7554/eLife.00049.022

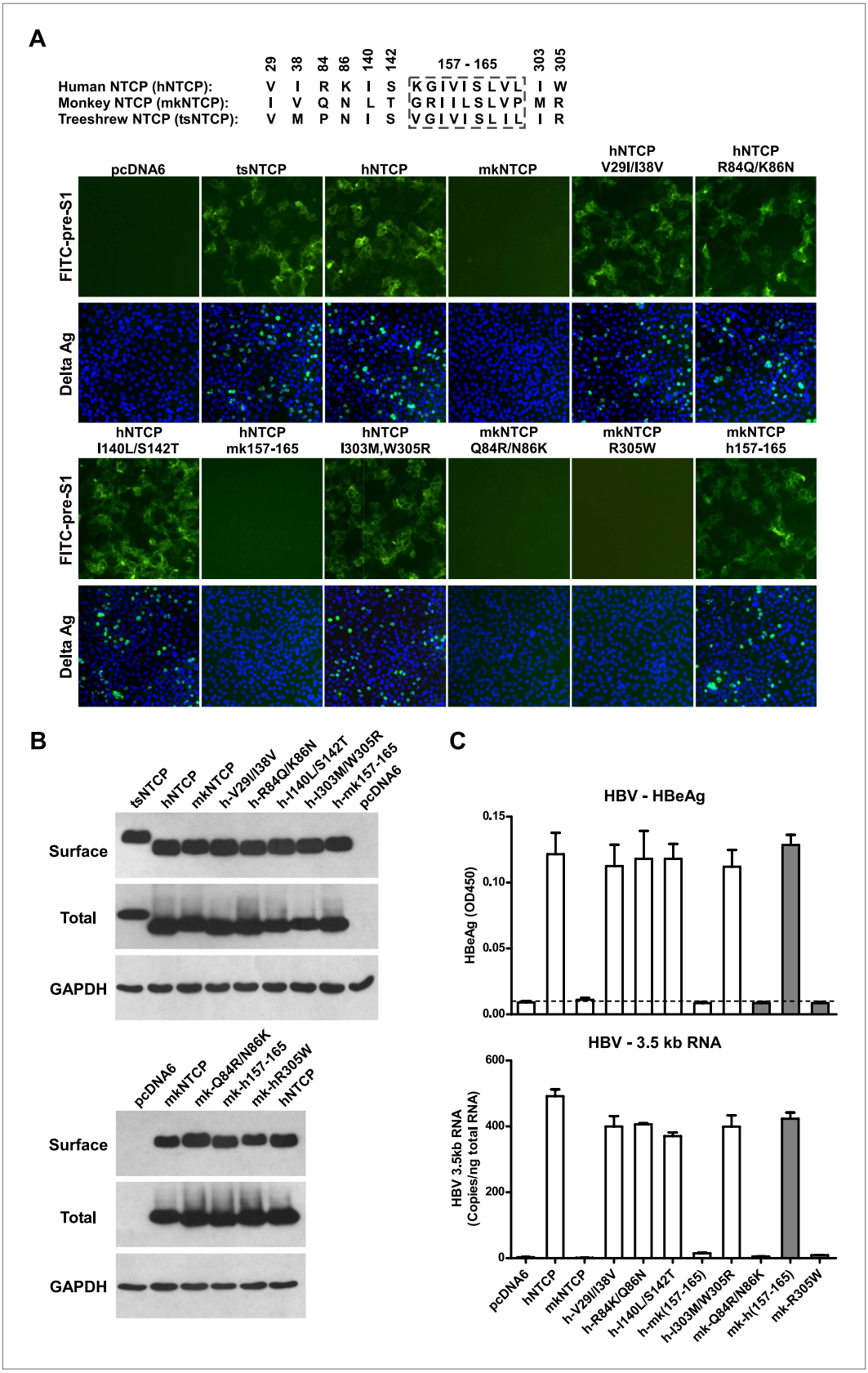

Figure 7. Identification of a critical region (aa 157–165) of NTCP for pre-S1 binding and viral infections. (**A**) Pre-S1 binding and HDV infection on cells expressing wild-type or mutant NTCPs. Corresponding amino acids (one-letter

Figure 7. Continued on next page

Figure 7 Continued

form) at the mutated positions of NTCP are shown for hNTCP, crab-eating monkey NTCP (mkNTCP), and tsNTCP. Huh-7 cells were transfected with plasmids encoding tsNTCP, hNTCP, mkNTCP, or NTCP mutants as indicated. The mutant NTCPs include hNTCP-bearing mutations of mkNTCP residues and mkNTCP-bearing mutations of human residues at indicated positions. The transfected cells were maintained in PMM for 24 hr and then either stained with 200 nM FITC-pre-S1 or infected with 500 mge HDV. HDV delta antigen in infected cells was detected with mAb 4G5 on 7 dpi. Replacing aa 157–165 of mkNTCP with human counterpart rendered mkNTCP an efficient receptor for pre-S1 binding and HDV infection. (**B**) All NTCP variants expressed comparable levels of NTCP. Huh-7 cells transfected as in panel A were biotinylated 24 hr after the transfection, then lysed and analyzed for cell surface NTCP expression (top), total NTCP expression (middle), and GAPDH (bottom), respectively. For cell surface expression, cell lysates were pulled down with streptavidin T1 Dynabeads and subsequently examined by western blot with mAb 1D4 recognizing a C9 tag at the C-terminus of each NTCP variant. For total NTCP expression, cell lysates were directly subjected to SDS-PAGE, followed by Western blot analysis with 1D4. (**C**) Effects of NTCP mutations on HBV infection. HepG2 cells were transfected with plasmids encoding hNTCP, mkNTCP, or hNTCP variants bearing the indicated monkey residues, or mkNTCP variants with the indicated human residues. Transfected cells were maintained in PMM for 24 hr, and subsequently infected with HBV at 100 mge. HBeAg and HBV 3.5 kb RNA were assayed on 6 dpi. Similar to panel B, comparable NTCP surface expression levels in the transfected HepG2 cells were confirmed for all the NTCP variants tested (***Figure 7—figure supplement 2***). NTCP: sodium taurocholate cotransporting polypeptide; HDV: hepatitis D virus; hNTCP: human NTCP; tsNTCP: *Tupaia* NTCP; PMM: primary hepatocytes maintenance medium; mge: multiplicities of genome equivalents; mAb: monoclonal antibody; HBV: hepatitis B virus; HBeAg: HBV e antigen; dpi: days post-infection.

DOI: 10.7554/eLife.00049.023

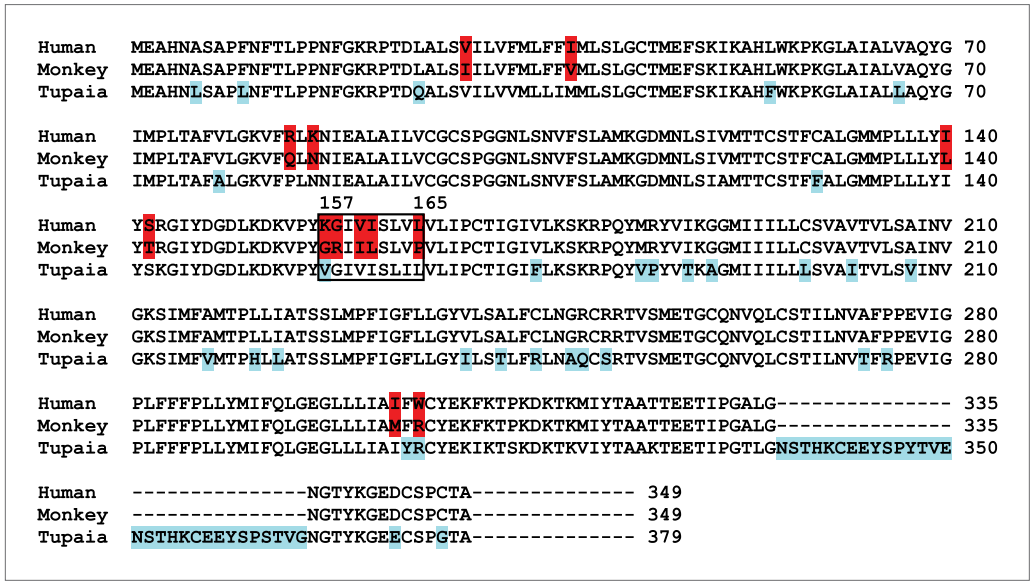

Figure 7—figure supplement 1. Protein sequence alignment of human, monkey, and *Tupaia* NTCP. Residues different between human and monkey are highlighted in red. *Tupaia* residues different from human's are in blue. Residues 157–165 are boxed.

DOI: 10.7554/eLife.00049.024

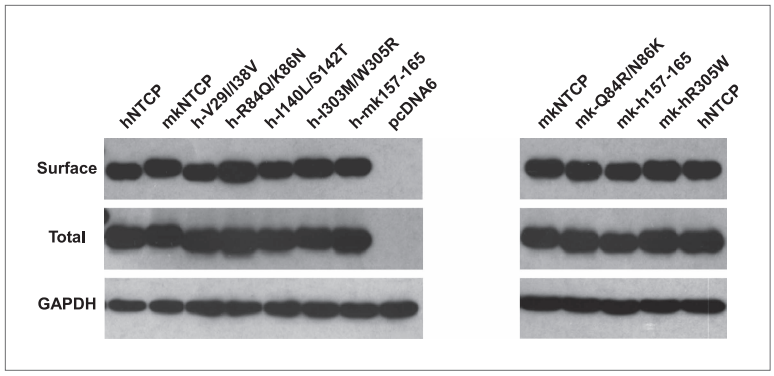

Figure 7—figure supplement 2. Total and surface NTCP expression levels in the transfected HepG2 cells. Transiently transfected HepG2 cells from the same batch of transfection as in ***Figure 7C*** were analyzed for total or cell surface NTCP expression at 24 hr post-transfection as described in ***Figure 7B***.

DOI: 10.7554/eLife.00049.025